International Journal of Control, Automation, and Systems (2011) 9(2):402-409 http://www.springer.com/12555
DOI 10.1007/s12555-011-0224-1

A Stability-Guaranteed Integral Sliding Disturbance Observer for Systems Suffering from Disturbances with Bounded First Time Derivatives

Yu-Sheng Lu and Chien-Wei Chiu

Abstract: This paper presents an integral sliding disturbance observer (I-SDOB) to compensate for unknown disturbances for a class of nonlinear systems. To guarantee the existence of a sliding mode for disturbance estimation, the proposed I-SDOB needs only a small switching gain compared with conventional sliding disturbance observers, which leads to further alleviation of chatter. Moreover, the stability analysis of the controller-observer system is given based on the Lyapunov theory. Applications of the proposed scheme to a two-link robotic manipulator have been conducted, and experimental results confirm the effectiveness of the proposed scheme.

Keywords: Disturbance observer, servo systems, sliding mode, stability.

1. INTRODUCTION

Disturbance observers are feasible tools to compensate for unknown disturbances and are widely adopted in motion control systems. In contrast to the high-gain feedback control, the compensator based on a disturbance observer estimates the unknown disturbance, and generates just minimal control to govern system dynamics to nominal dynamics. The structures of disturbance observers can be divided into four main categories. One category [1-3] uses the time-delayed estimation technique and requires the information on the time derivative of state vector, to which the access is however usually contaminated with noise in most practical implementations. The second category [4-6] requires the knowledge of system parameters to construct a disturbance observer free from the necessity of evaluating the time derivative of state vector. Increasing the bandwidth of the disturbance observer could enforce its transient performance but decreases its immunity against noise. As an extreme case, the disturbance observer with a bandwidth of infinity implicitly differentiates the state vector with respect to time. The third category [7-9] adopted structures similar to a state estimator, employed the technique of appending a disturbance state to the conventional state observer, and assumed that the time variation of an unknown disturbance is zero. The last category [10-16] is related to designing a sliding disturbance observer. Due to the inherent invariance property of a sliding mode, a sliding state observer possesses design simplicity and favorable robustness against modeling errors and disturbances. It is thus natural to apply the structure of a sliding state observer to designing a sliding disturbance observer such that the estimation process is robust to system perturbations.

Concerning disturbance estimation using a sliding disturbance observer, the estimate of disturbance in [10] contains switching components which, when introduced to disturbance compensation, may excite unmodeled dynamics and lead to oscillations in state vector at finite frequency. These oscillations, normally referred to as chatter, are known to result in low-control accuracy, high heat loss in electric power circuit, and high wear of moving mechanical parts [14]. A smooth saturation-type function is adopted in [11,12] to approximate the discontinuous function, alleviating control chatter at the sacrifice of estimation precision. Moreover, the analysis in [12] assumed that the time variation of disturbance has negligible effect. In [13-16], the disturbance is shown to be equal to the equivalent value of some switching signal, and its estimate is obtained by feeding the switching signal through a low-pass filter. It was stated in [17] that the equivalent value is equal to the average value measured by a first-order linear filter with switched actions as its input if the time constant of this filter is coordinated with the width of the area where motion in sliding mode takes place. However, this kind of filter with its bandwidth instantly adapted according to the situation of real sliding motion is almost unrealizable in practice. By using a fixed-bandwidth low-pass filter with the switching signal as its input for disturbance estimation, there exists trade-off between the estimation precision and the chatter. This means that, when the bandwidth of the filter is increased, the equivalent value of the switching signal is better preserved in the low-frequency range, yielding more precise estimation but leading to more chatter. On the other hand, decreasing the bandwidth of the filter alleviates chatter but distorts

Manuscript received September 7, 2008; revised January 23, 2010; accepted November 15, 2010. Recommended by Editor Young Il Lee. This work was supported by the National Science Council of ROC under grant NSC 98-2221-E-003-008-MY2.

Yu-Sheng Lu is with the Department of Mechatronic Technology, National Taiwan Normal University, 162, He-ping East Rd., Sec. 1, Taipei 106, Taiwan (e-mail: luys@ntnu.edu.tw).

Chien-Wei Chiu with the Department of Mechanical Engineering, National Yunlin University of Science and Technology, 123, University Road, Section 3, Touliu, Yunlin 640, Taiwan (e-mail: g9211723@yuntech.edu.tw).

the equivalent value, giving poorer disturbance estimation. Moreover, switching gains in these designs must be greater than the bounds on disturbances. Large switching gains imply significant chatter.

In [18], the conventionally assumed upper bound restriction on the disturbance is relaxed to the restriction on its estimation error, thus requiring a much smaller switching gain to ensure the existence of a sliding mode. Through this reduction of a switching gain together with the low-pass filtering characteristics of the estimation process, the chatter problem is further alleviated without the sacrifice of estimation precision. Nevertheless, the stability of the overall system in [18] is not ensured. Moreover, only single-input single-output systems are considered in [18]. This paper proposes the design of an integral sliding disturbance observer (I-SDOB) that both requires only a small switching gain and also guarantees stability of the disturbance-compensated system. Besides, this paper deals with a class of nonlinear multiple-input multiple-output systems. To demonstrate its effectiveness, the proposed design is applied to a two-link robotic manipulator with various payloads.

2. AN INTEGRAL SLIDING DISTURBANCE OBSERVER (I-SDOB)

Consider fully-actuated Euler-Lagrange mechanical systems described by

$$\mathbf{M}(\mathbf{q})\ddot{\mathbf{q}} + \mathbf{B}(\mathbf{q},\dot{\mathbf{q}})\dot{\mathbf{q}} + \mathbf{g}(\mathbf{q}) = \mathbf{u}(t) + \mathbf{d}(t), \tag{1}$$

in which $\mathbf{q} \in R^n$ is the vector of Lagrangian coordinates, $\mathbf{u} \in R^n$ is the vector of generalized control torques, $\mathbf{M}(\mathbf{q})$ is the $n \times n$ symmetric inertia matrix being positive definite, $\mathbf{B}(\mathbf{q},\dot{\mathbf{q}})$ is the $n \times n$ matrix containing Coriolis and centripetal terms, and $\mathbf{g}(\mathbf{q}) \in R^n$ is the gravitational torque vector. Here, $\mathbf{d}(t) \in R^n$ denotes unknown lumped disturbances, including external disturbances and the effect of modeling uncertainties referred to the actuator inputs. Define the tracking error as $\mathbf{e}=\mathbf{q}-\mathbf{q}_r$, in which $\mathbf{q}_r$ denotes the reference trajectory assumed to be twice differentiable with respect to time. Moreover, define a filtered error vector $\mathbf{s}$ to be

$$\mathbf{s} = \dot{\mathbf{e}} + \mathbf{C}\mathbf{e}, \tag{2}$$

in which $\mathbf{C} = \mathrm{diag}[c_1, c_2, \cdots, c_n]$, and $c_i > 0$ for $i = 1, 2, \cdots, n$. Let the control be in an additive form

$$\mathbf{u} = \mathbf{u}_n - \hat{\mathbf{d}}, \tag{3}$$

in which $\hat{\mathbf{d}}$ denotes the disturbance estimate by a disturbance observer, and the nominal control $\mathbf{u}_n$ is described by

$$\mathbf{u}_n = \mathbf{M}\dot{\mathbf{v}} + \mathbf{B}\mathbf{v} + \mathbf{g} - \mathbf{\Phi}\mathbf{s}, \tag{4}$$

in which $\mathbf{v} = \dot{\mathbf{q}}_r - \mathbf{C}\mathbf{e}$, and the parameter matrix $\mathbf{\Phi} = \mathrm{diag}[\phi_1, \phi_2, \cdots, \phi_n]$ with $\phi_i > 0$ for $i = 1, 2, \cdots, n$. Taking the time derivative of (2), multiplying it by $\mathbf{M}(\mathbf{q})$, and substituting (1), (3) and (4) into the resulting equation gives

$$\begin{aligned}\mathbf{M}\dot{\mathbf{s}} &= \mathbf{M}(\ddot{\mathbf{q}} - \dot{\mathbf{v}}) = -\mathbf{B}\dot{\mathbf{q}} - \mathbf{g} + \mathbf{u}_n - \hat{\mathbf{d}} + \mathbf{d} - \mathbf{M}\dot{\mathbf{v}} \\ &= -\mathbf{B}\dot{\mathbf{q}} + \mathbf{B}\mathbf{v} - \mathbf{\Phi}\mathbf{s} - \hat{\mathbf{d}} + \mathbf{d} = -\mathbf{B}\mathbf{s} - \mathbf{\Phi}\mathbf{s} + \mathbf{d} - \hat{\mathbf{d}}.\end{aligned} \tag{5}$$

Consider a Lyapunov candidate

$$2V_n = \mathbf{s}^T\mathbf{M}\mathbf{s}. \tag{6}$$

Taking the time derivative of (6) and substituting (5) into the resulting equation gives

$$\begin{aligned}\dot{V}_n &= \mathbf{s}^T\mathbf{M}\dot{\mathbf{s}} + \frac{1}{2}\mathbf{s}^T\dot{\mathbf{M}}\mathbf{s} \\ &= \mathbf{s}^T(-\mathbf{B}\mathbf{s} - \mathbf{\Phi}\mathbf{s} + \mathbf{d} - \hat{\mathbf{d}}) + \mathbf{s}^T\mathbf{B}\mathbf{s} \\ &= -\mathbf{s}^T\mathbf{\Phi}\mathbf{s} + \mathbf{s}^T(\mathbf{d} - \hat{\mathbf{d}}),\end{aligned} \tag{7}$$

in which the property of $\dot{\mathbf{M}}(\mathbf{q}) = \mathbf{2B}(\mathbf{q},\dot{\mathbf{q}}) + \mathbf{J}(\mathbf{q},\dot{\mathbf{q}})$ has been employed. Here, $\mathbf{J}(\mathbf{q},\dot{\mathbf{q}})$ is a skew-symmetric matrix of appropriate dimension. In the ideal situation when $\hat{\mathbf{d}} = \mathbf{d}$, we have $\dot{V}_n = -\mathbf{s}^T\mathbf{\Phi}\mathbf{s}$, showing the negative definiteness of $\dot{V}_n$ and thus guaranteeing the asymptotic convergence of the error vector $\mathbf{e}$.

An integral sliding disturbance observer (I-SDOB) is to be designed to generate $\hat{\mathbf{d}}$ in order to compensate for the disturbance $\mathbf{d}$. Consider an artificially introduced auxiliary process described by

$$\mathbf{M}\dot{\mathbf{z}} = -\mathbf{B}\dot{\mathbf{q}} - \mathbf{g} + \mathbf{u} + \hat{\mathbf{d}} - \mathbf{B}\mathbf{\sigma} - \mathbf{\Psi}\,\mathrm{sgn}(\mathbf{\sigma}), \tag{8}$$

in which $\mathbf{z} \in R^n$ is the state vector of the auxiliary process, the switching function $\mathbf{\sigma} = \mathbf{z} - \dot{\mathbf{q}}$, sgn(·) denotes the sign function, the switching gain $\mathbf{\Psi} = \mathrm{diag}[\psi_1, \psi_2, \cdots, \psi_n]$, and $\psi_i > 0$ for $i = 1, 2, \cdots, n$. Subtracting (1) from (8), one has

$$\mathbf{M}\dot{\mathbf{\sigma}} = -\mathbf{d} + \hat{\mathbf{d}} - \mathbf{B}\mathbf{\sigma} - \mathbf{\Psi}\,\mathrm{sgn}(\mathbf{\sigma}). \tag{9}$$

To verify the existence of the sliding mode $\mathbf{\sigma}(t) = \mathbf{0}$, consider a Lyapunov candidate

$$2V_o = \mathbf{\sigma}^T\mathbf{M}\mathbf{\sigma}. \tag{10}$$

Taking the time derivative of (10) and substituting (9) into the resulting equation gives

$$\begin{aligned}\dot{V}_o &= \mathbf{\sigma}^T\mathbf{M}\dot{\mathbf{\sigma}} + \frac{1}{2}\mathbf{\sigma}^T\dot{\mathbf{M}}\mathbf{\sigma} \\ &= \mathbf{\sigma}^T(-\mathbf{d} + \hat{\mathbf{d}} - \mathbf{B}\mathbf{\sigma} - \mathbf{\Psi}\,\mathrm{sgn}(\mathbf{\sigma})) \\ &\quad + \mathbf{\sigma}^T\mathbf{B}\mathbf{\sigma} = \mathbf{\sigma}^T(-\mathbf{d} + \hat{\mathbf{d}} - \mathbf{\Psi}\,\mathrm{sgn}(\mathbf{\sigma})).\end{aligned} \tag{11}$$

Provided that $\psi_i > |d_i - \hat{d}_i|$ for $i = 1, 2, \cdots, n$, in which d_i and $\hat{d}_i$ denote the ith components of $\mathbf{d}$ and $\hat{\mathbf{d}}$, respectively, then $\dot{V}_o$ is negative definite, ensuring the satisfaction of the so-called sliding condition, which guarantees the existence of the sliding mode $\mathbf{\sigma}(t) = \mathbf{0}$ when the representative point is close to the sliding

regime. A disturbance can be considered to be composed of low-frequency and high-frequency components. In practical applications, the low-frequency components of a disturbance are often much larger in magnitude than its high-frequency components; e.g., the dc component usually has the largest magnitude. Since the low-frequency components of a disturbance can be easily and precisely estimated by a disturbance observer, the magnitude of the estimation error $|d_i - \hat{d}_i|$ can be kept small compared with the magnitude of the original disturbance that mostly contains low-frequency components. In the previous sliding disturbance observers [10-16], the switching gain must be greater than the magnitude of the disturbance to ensure the fulfillment of the sliding condition. In the proposed I-SDOB, the switching gain ψ_i needs only to be greater than the magnitude of the estimation error $|d_i - \hat{d}_i|$, reducing the required magnitude of a switching gain and thus further alleviating the chatter.

By setting the initial state of the auxiliary process $\mathbf{z}(0) = \dot{\mathbf{q}}(0)$, one obtains $\boldsymbol{\sigma}(0) = \mathbf{0}$. This together with the negative definiteness of $\dot{V}_o$ yields $\boldsymbol{\sigma}(t) = \mathbf{0}$ for $t \geq 0$, demonstrating that the sliding mode $\boldsymbol{\sigma} = \mathbf{0}$ exists throughout an entire response. Since $\boldsymbol{\sigma}(t) = \mathbf{0}$, one has $\dot{\boldsymbol{\sigma}}(t) = \mathbf{0}$ that further gives from (9)

$$\mathbf{d} - \hat{\mathbf{d}} = -\boldsymbol{\Psi}\,\mathrm{sgn}(\boldsymbol{\sigma}) - \mathbf{B}\boldsymbol{\sigma}, \tag{12}$$

in the sense of equivalent values [17]. Consider the following integral law for disturbance estimation

$$\dot{\hat{\mathbf{d}}} = \mathbf{K}_d\left[-\boldsymbol{\Psi}\,\mathrm{sgn}(\boldsymbol{\sigma}) - \mathbf{B}\boldsymbol{\sigma}\right] + k_s\mathbf{s}, \tag{13}$$

in which $\mathbf{K}_d = \mathrm{diag}[k_{d1}, k_{d2}, \cdots, k_{dn}]$, $k_{di} > 0$ for $i = 1, 2, \cdots, n$, and $k_s > 0$. Fig. 1 shows the schematic diagram of the proposed approach. To confirm the stability of the overall controller-observer system, consider a Lyapunov function

$$V_s = \frac{1}{2}k_s\mathbf{s}^T\mathbf{M}\mathbf{s} + \frac{1}{2}(\mathbf{d} - \hat{\mathbf{d}})^T(\mathbf{d} - \hat{\mathbf{d}}), \tag{14}$$

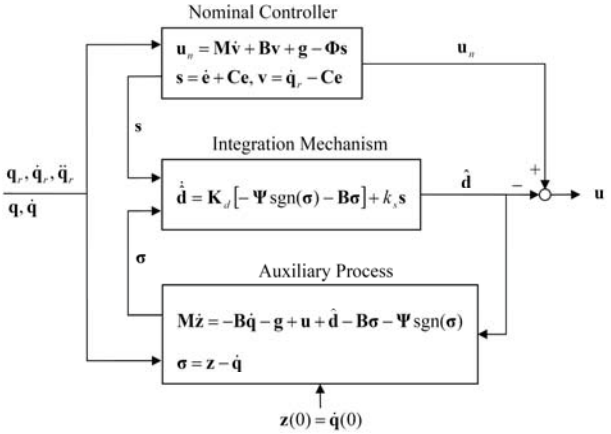

Fig. 1. Block diagram of the proposed control scheme.

which is radially unbounded. Similar to (7), the time derivative of the first term on the right-hand side of (14) can be derived as

$$\frac{1}{2}\frac{d}{dt}\left(k_s\mathbf{s}^T\mathbf{M}\mathbf{s}\right) = -k_s\mathbf{s}^T\boldsymbol{\Phi}\mathbf{s} + k_s\mathbf{s}^T(\mathbf{d} - \hat{\mathbf{d}}). \tag{15}$$

Furthermore, taking the time derivative of the second term on the right-hand side of (14) and using (12) and (13), one has

$$\begin{aligned}&\frac{1}{2}\frac{d}{dt}\left[(\mathbf{d} - \hat{\mathbf{d}})^T(\mathbf{d} - \hat{\mathbf{d}})\right]\\ &= (\mathbf{d} - \hat{\mathbf{d}})^T\dot{\mathbf{d}} - (\mathbf{d} - \hat{\mathbf{d}})^T\dot{\hat{\mathbf{d}}}\\ &= (\mathbf{d} - \hat{\mathbf{d}})^T\dot{\mathbf{d}} - (\mathbf{d} - \hat{\mathbf{d}})^T\mathbf{K}_d(\mathbf{d} - \hat{\mathbf{d}}) - k_s(\mathbf{d} - \hat{\mathbf{d}})^T\mathbf{s}.\end{aligned} \tag{16}$$

Combining (15) and (16) gives

$$\dot{V}_s = -k_s\mathbf{s}^T\boldsymbol{\Phi}\mathbf{s} - (\mathbf{d} - \hat{\mathbf{d}})^T\mathbf{K}_d(\mathbf{d} - \hat{\mathbf{d}}) + (\mathbf{d} - \hat{\mathbf{d}})^T\dot{\mathbf{d}}. \tag{17}$$

Using the fact that $-(\gamma_1 k_{di}(d_i - \hat{d}_i) - \dot{d}_i/2)^2 \leq 0$, in which γ_1 is a positive constant, one has

$$-\gamma_1^2 k_{di}^2(d_i - \hat{d}_i)^2 + \gamma_1 k_{di}(d_i - \hat{d}_i)\dot{d}_i - \dot{d}_i^2/4 \leq 0. \tag{18}$$

Assume that the first time derivative of disturbances is bounded, i.e., $|\dot{d}_i| \leq D_i$ for $i = 1, 2, \cdots, n$, in which D_i is an upper bound on $|\dot{d}_i|$. Then, (18) further gives

$$-\gamma_1 k_{di}(d_i - \hat{d}_i)^2 + (d_i - \hat{d}_i)\dot{d}_i \leq \frac{\dot{d}_i^2}{4\gamma_1 k_{di}} \leq \frac{D_i^2}{4\gamma_1 k_{di}}. \tag{19}$$

Let $\mathbf{K}_d = (\gamma_0 + \gamma_1)\mathbf{K}_d$, in which $\gamma_0 + \gamma_1 = 1$, $\gamma_0 > 0$, and $\gamma_1 > 0$. Using this relation and (19) yields

$$\dot{V}_s \leq -k_s\mathbf{s}^T\boldsymbol{\Phi}\mathbf{s} - \gamma_0(\mathbf{d} - \hat{\mathbf{d}})^T\mathbf{K}_d(\mathbf{d} - \hat{\mathbf{d}}) + \delta, \tag{20}$$

where $\delta = \sum_{i=1}^{n} D_i^2/4\gamma_1 k_{di}$. Define $\lambda_{\Phi\min} = \min\{\phi_i\}_{i=1}^n$ and $\lambda_{\mathrm{Kd}\min} = \min\{k_{di}\}_{i=1}^n$, which represent the smallest eigenvalues of $\boldsymbol{\Phi}$ and $\mathbf{K}_d$, respectively. Rewrite (20) as

$$\dot{V}_s \leq -k_s\lambda_{\Phi\min}\|\mathbf{s}\|^2 - \gamma_0\lambda_{\mathrm{Kd}\min}\left\|\mathbf{d} - \hat{\mathbf{d}}\right\|^2 + \delta. \tag{21}$$

Finally, one obtains

$$\dot{V}_s < 0 \quad \text{when} \quad \mathbf{s} \notin \Omega_s \quad \text{or} \quad (\mathbf{d} - \hat{\mathbf{d}}) \notin \Omega_d, \tag{22}$$

in which $\Omega_d = \left\{\mathbf{d} - \hat{\mathbf{d}} \;\middle|\; \left\|\mathbf{d} - \hat{\mathbf{d}}\right\| \leq \sqrt{\frac{\delta}{\gamma_0\lambda_{\mathrm{Kd}\min}}}\right\}$, and $\Omega_s = \left\{\mathbf{s} \;\middle|\; \|\mathbf{s}\| \leq \sqrt{\frac{\delta}{k_s\lambda_{\Phi\min}}}\right\}$. The sets, Ω_s and Ω_d, represent two regions in the hyperspace $(\mathbf{s}, \mathbf{d} - \hat{\mathbf{d}})$. The result (22) shows that, when $\mathbf{s} \notin \Omega_s$ or $(\mathbf{d} - \hat{\mathbf{d}}) \notin \Omega_d$, the time derivative of the Laypunov function is negative definite. This means that the representative point $(\mathbf{s}, \mathbf{d} - \hat{\mathbf{d}})$ will

eventually enter a region that is the intersection of Ω_s and Ω_d. Since the intersection of Ω_s and Ω_d is a compact set in the hyperspace $(\mathbf{s}, \mathbf{d}-\hat{\mathbf{d}})$, the result (22) implies the global stability of the controller-observer system. From the definition of Ω_s and Ω_d, it is seen that the intersection of Ω_s and Ω_d shrinks when the values of controller-observer parameters increase. Thus, the upper bounds on the filtered tracking error $\mathbf{s}$ and the compensation error $(\mathbf{d}-\hat{\mathbf{d}})$ decrease with increased k_s and λ_{kdmin}, meaning that increasing k_s and $\mathbf{K}_d$ of the I-SDOB can improve the tracking and the estimation precision. When the unknown disturbance is time-invariant, i.e., D_i's are equal to zero, then $\delta = 0$, $\dot{V}_s$ is negative definite, and the equilibrium at the origin of the hyperspace $(\mathbf{s}, \mathbf{d}-\hat{\mathbf{d}})$ is globally asymptotically stable; that is, the I-SDOB completely rejects the unknown constant disturbance $\mathbf{d}$, and the tracking error asymptotically converges to zero.

Remark 1: There are two main differences between the proposed scheme and the previous one in [18]. One difference is that the proposed scheme ensures the stability of the overall system through Lyapunov analysis whereas the previous scheme [18] does not. The other difference is that the proposed design deals with multiple-input multiple-output nonlinear systems whereas the previous design [18] only handles single-input single-output linear systems. Although both disturbance estimation laws are of the integral form, their integrands are different. The proposed law introduces some additional terms into the integrand of the previous law, such as the term $k_s\mathbf{s}$ in (13), so as to ensure the stability of the overall system.

Remark 2: The choice of $\mathbf{K}_d$ and k_s in the I-SDOB is not unique. According to (13), the switching signal $\mathbf{\Psi}\text{sgn}(\boldsymbol{\sigma})$ is equivalent to the disturbance estimation error. Whenever the estimation error is not null, the switching signal excites the integration process (13) to estimate the disturbance. Roughly speaking, with larger eigenvalues of $\mathbf{K}_d$, the estimation error converges faster. On the other hand, increasing k_s increases the convergence rate of the filtered tracking error $\mathbf{s}$. Theoretically, any strictly positive k_s and $\mathbf{K}_d$ with strictly positive eigenvalues can stabilize the system. Moreover, according to the Laypunov analysis, larger k_s and $\mathbf{K}_d$ leads to smaller tracking and estimation errors. However, some physical constraints would limit the admissible values of k_s and $\mathbf{K}_d$, such as measurement noise, actuator saturation, digital implementation, and the existence of unmodeled plant dynamics.

3. AN APPLICATION TO A TWO-LINK ROBOTIC MANIPULATOR

3.1. Plant description and system model

Consider the position control of a two-link revolute-joint manipulator subject to an unknown constant payload. For a two-link robot manipulator moving in the vertical plane as shown in Fig. 2, the dynamic equation is given by

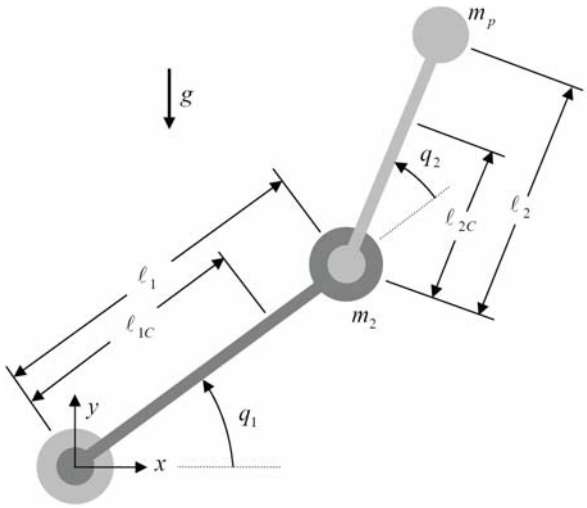

Fig. 2. Experimental planar robot manipulator.

$$\begin{bmatrix} M_{11} & M_{12} \\ M_{21} & M_{22} \end{bmatrix}\begin{bmatrix} \ddot{q}_1 \\ \ddot{q}_2 \end{bmatrix}+\begin{bmatrix} B_{11} & B_{12} \\ B_{21} & B_{22} \end{bmatrix}\begin{bmatrix} \dot{q}_1 \\ \dot{q}_2 \end{bmatrix}+\begin{bmatrix} g_1 \\ g_2 \end{bmatrix} = \begin{bmatrix} u_1+d_1 \\ u_2+d_2 \end{bmatrix}, \tag{23}$$

in which

$$\begin{aligned}
M_{11} &= m_{\ell 1}\ell_{1c}^2 + I_{\ell 1} + I_{m1} + (m_{\ell 2}+m_2+m_p)\ell_1^2 \\
&\quad + m_{\ell 2}\ell_{2c}^2 + I_{\ell 2} + I_{m2} + I_{M2} + m_p\ell_2^2 \\
&\quad + 2(m_{\ell 2}\ell_{2c} + m_p\ell_2)\ell_1\cos q_2, \\
M_{12} &= M_{21} \\
&= m_{\ell 2}\ell_{2c}^2 + I_{\ell 2} + I_{m2} + m_p\ell_2^2 \\
&\quad + (m_{\ell 2}\ell_{2c} + m_p\ell_2)\ell_1\cos q_2, \\
M_{22} &= m_{\ell 2}\ell_{2c}^2 + I_{\ell 2} + I_{m2} + m_p\ell_2^2, \\
B_{11} &= -2(m_{\ell 2}\ell_{2c} + m_p\ell_2)\ell_1\dot{q}_2\sin q_2, \\
B_{12} &= -(m_{\ell 2}\ell_{2c} + m_p\ell_2)\ell_1\dot{q}_2\sin q_2, \\
B_{21} &= (m_{\ell 2}\ell_{2c} + m_p\ell_2)\ell_1\dot{q}_1\sin q_2, \\
B_{22} &= 0, \quad g_2 = g[(m_{\ell 2}\ell_{2c} + m_p\ell_2)\cos(q_1+q_2)], \\
g_1 &= g[(m_{\ell 1}\ell_{1c} + m_{\ell 2}\ell_1 + m_2\ell_1 + m_p\ell_1)\cos q_1 \\
&\quad + (m_{\ell 2}\ell_{2c} + m_p\ell_2)\cos(q_1+q_2)].
\end{aligned}$$

Here, $m_{\ell i}$ is the mass of link i, $I_{\ell i}$ is its moment of inertia about mass centre, ℓ_i denotes the length of link i, ℓ_{ic} is the distance between the joint i and the mass centre of link i, I_{mi} is the rotor moment of inertia of motor i, I_{M2} is the stator moment of inertia of motor 2, m_2 is the mass of motor 2, g is the gravitation constant, and m_p denotes the mass of the unknown constant payload.

The robot in the experimental setup is directly driven by two permanent-magnet ac servomotors. Fig. 3 shows the configuration of the robot control system, in which ac motors 1 and 2 are with rated output power of 400 W and 100 W, respectively, and both are SGMAH Servomotors manufactured by Yaskawa Electric. The control inputs

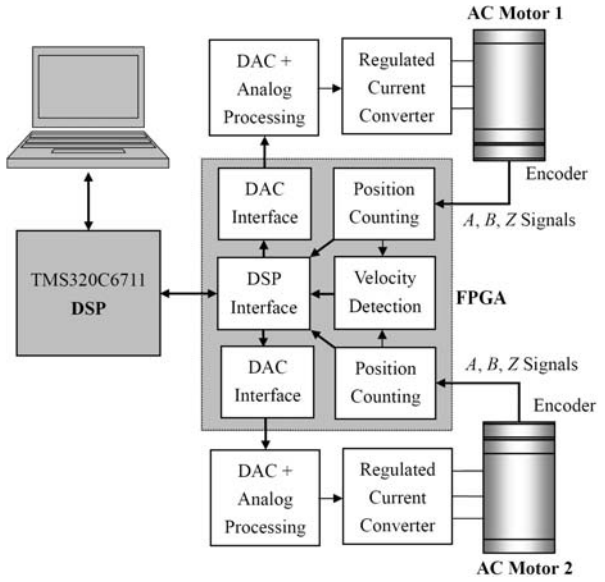

Fig. 3. Hardware configuration of the control system.

are constrained by $|u_1(t)| \le 1.4$ (N·m) and $|u_2(t)| \le 0.3$ (N·m). The shaft encoder mounted to each ac servomotor has 2,048 lines, which yields a resolution of 8,192 pulses/rev after the A and B signals from the encoder have been processed by the FPGA (Field- Programmable Gate Array), model XCV50PQ240-C6 from Xilinx, Inc. The velocity information is measured by a digital tachometer that measures the time interval of the encoder pulses to achieve more accurate estimation than the direct differentiation of the position signal. The tasks of both position counting and velocity detection are implemented in the FPGA. The controller core is a floating-point TMS320C6711 digital signal processor (DSP) that executes an ISR at a rate of 12.2 kHz. In that ISR, the DSP obtains information on position and velocity from the FPGA, calculates control algorithms, and sends control efforts to regulated current converters through 12-bit digital-to-analog converters and some analog signal processing circuits. In the experimental system, a personal computer was used to develop the control program written in C language, to compile it, to download the resulting code into DSP for execution, and to acquire experimental data. Estimated parameter values of the robot are $m_{\ell 1} = 0.064$, $m_{\ell 2} = 0.039$, $I_{\ell 1} = 1.93 \times 10^{-4}$, $I_{\ell 2} = 6.63 \times 10^{-5}$, $\ell_1 = 0.117$, $\ell_2 = 0.105$, ℓ_{1c} =0.055, $\ell_{2c} = 0.037$, $I_{m1} = 6.16 \times 10^{-5}$, $I_{m2} = 3.64 \times 10^{-6}$, I_{M2} =1.8× 10^{-4}, and $m_2 = 0.54$ in SI units. The main system uncertainties are due to the payload and external disturbances including joint frictions. In the following experiments, various payloads with known mass, i.e., $m_p = 0.1$, $m_p = 0.2$, and $m_p = 0.3$ (kg), are employed to test the performance of the proposed scheme. Since the range of the payload is between 0.1 kg and 0.3 kg, its nominal value $\hat{m}_p = (0.3 + 0.1)/2 = 0.2$ (kg) is then used in the controller/observer design. Note that the nominal value $\hat{m}_p$ in the controller/observer is fixed in spite of payload changes.

3.2. Controller/observer design and experimental results

According to (3), the control law in an additive form is $\mathbf{u} = \mathbf{u}_n - \hat{\mathbf{d}}$. The nominal control is given by $\mathbf{u}_n = \mathbf{M}\dot{\mathbf{v}} + \mathbf{B}\mathbf{v} + \mathbf{g} - \mathbf{\Phi}\mathbf{s}$, in which $\mathbf{v} = \dot{\mathbf{q}}_r - \mathbf{C}\mathbf{e}$, $\mathbf{s} = \dot{\mathbf{e}} + \mathbf{C}\mathbf{e}$, $\mathbf{C} = \text{diag}[10, 10]$, and $\mathbf{\Phi} = \text{diag}[0.2, 0.06]$. For the I-SDOB, the artificially introduced auxiliary process is described by $\mathbf{M}\dot{\mathbf{z}} = -\mathbf{B}\dot{\mathbf{q}} - \mathbf{g} + \mathbf{u} + \hat{\mathbf{d}} - \mathbf{B}\boldsymbol{\sigma} - \mathbf{\Psi}\,\text{sgn}(\boldsymbol{\sigma})$, in which $\mathbf{z}(0) = \dot{\mathbf{q}}(0)$, $\boldsymbol{\sigma} = \mathbf{z} - \dot{\mathbf{q}}$, and $\mathbf{\Psi} = \text{diag}[0.2, 0.2]$. Then, the integral law for disturbance estimation is $\dot{\hat{\mathbf{d}}} = \mathbf{K}_d \left[-\mathbf{\Psi}\,\text{sgn}(\boldsymbol{\sigma}) - \mathbf{B}\boldsymbol{\sigma} \right] + k_s \mathbf{s}$, in which $\mathbf{K}_d$=diag[20, 20] and $k_s = 0.01$. In the following experiments, discontinuous step references and a continuously time-varying reference were examined, and the plant was initially at rest, i.e., $\mathbf{q}(0) = [-\pi/2 \quad 0]^T$ (rad) and $\dot{\mathbf{q}}(0) = [0 \quad 0]^T$.

Consider the following reference in radians

$$\mathbf{q}_r(t) = \mathbf{q}(0) + H(t)[1 \quad 1]^T, \tag{24}$$

in which $H(\cdot)$ denotes an unit-step function. Fig. 4

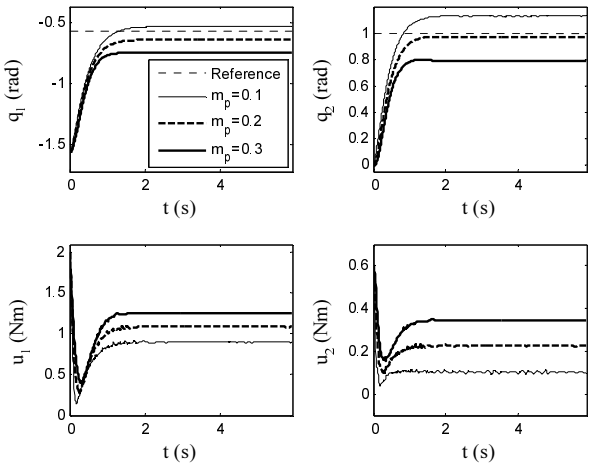

Fig. 4. Step responses with various payloads by the nominal control.

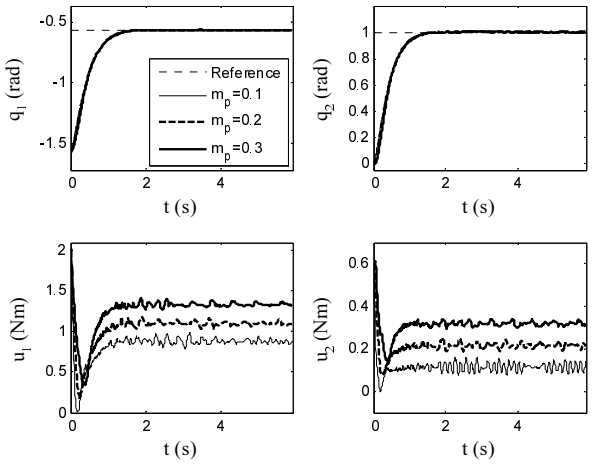

Fig. 5. Step responses with various payloads by the proposed control.

shows the dynamic responses with various payloads by the nominal control without disturbance compensation, i.e., $\mathbf{u}=\mathbf{u}_n$. It is seen that the performance with the nominal control is sensitive to the variations of payload. Fig. 5 shows the dynamic responses with various payloads by the proposed control, demonstrating that the output responses are almost invariant to the payload variations. Furthermore, consider the following reference trajectory in radians

$$\mathbf{q}_r(t) = \mathbf{q}(0) + [H(t-2) - H(t-4) \quad H(t) - H(t-4)]^T, \tag{25}$$

in which the second link is required to move a displacement of 1 rad at the beginning, the first link is afterwards commanded to rotate 1 rad at 2 s, and finally both links start to move toward the initial position at 4 s. Fig. 6 shows the dynamic responses subject to payload variations and by the nominal control only, demonstrating that the output performance is much influenced by the payload variations. It is also seen that the system with the payload of 0.3 kg exhibits output overshoot when returning to the initial position $\mathbf{q}(0)$. Fig. 7 presents the dynamic responses with different payloads by the proposed control, showing that the disturbance compensation by the I-SDOB greatly improves system robustness and yields almost zero-overshooting output responses.

To investigate tracking performance in a Cartesian coordinate system defined in Fig. 2, consider the following reference trajectory for the end effector of the robotic manipulator

$$\begin{cases} x_r = 0.08 + r(1 - \sin(\omega t + \varphi)\cos(\omega t + \varphi), \\ y_r = -0.08 + r(1 - \sin(\omega t + \varphi))\cos(\omega t + \varphi), \end{cases} \tag{26}$$

in which $r = 0.05$ (m), $\varphi = 3\pi/2$ (rad), and $\omega = -1.278$ (rad/s). Note that the origin of the stationary Cartesian coordinate system is located at the rational center of motor 1, and the initial position of the end effector associated with $\mathbf{q}(0)$ is at $(x(0), y(0)) = (0, -\ell_1 - \ell_2)$. The desired trajectory in the joint space is obtained through the inverse kinematics of this manipulator. Fig. 8 depicts the dynamic responses with various payloads by the nominal control, illustrating that the nominal control alone cannot yield adequate tracking performance. Fig. 9 shows the dynamic responses with various payloads by

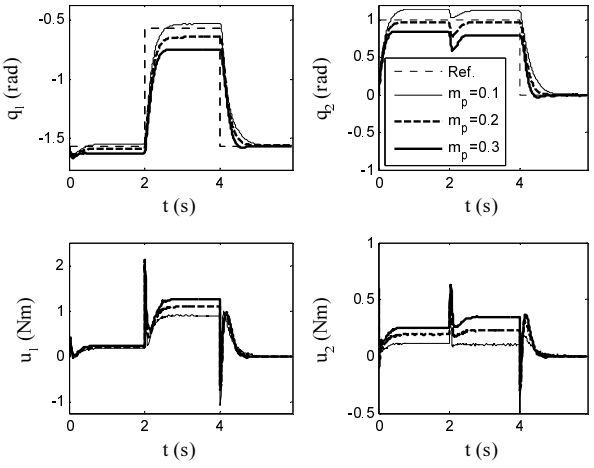

Fig. 6. Dynamic responses with various payloads by the nominal control.

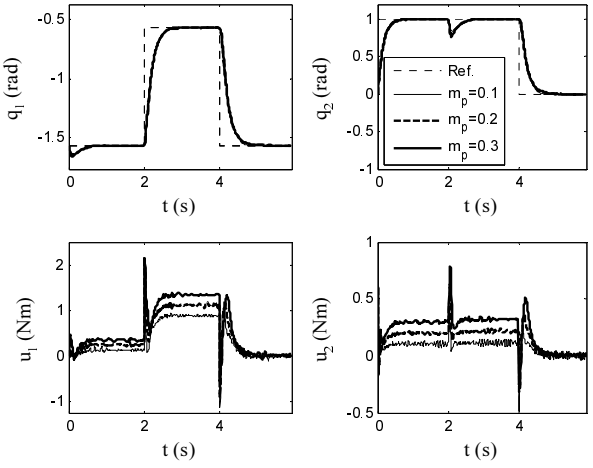

Fig. 7. Dynamic responses with various payloads by the proposed control.

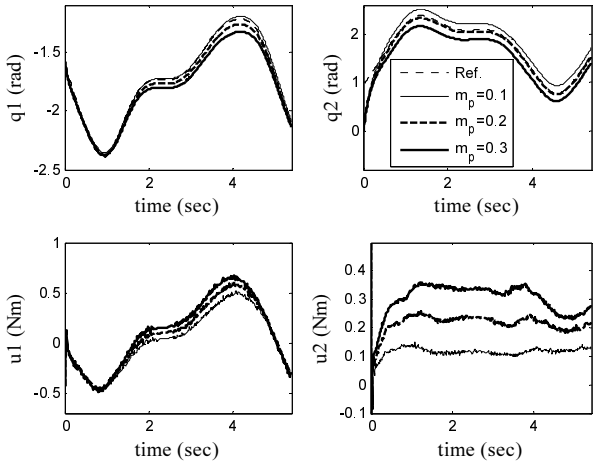

Fig. 8. Tracking responses with various payloads by the nominal control.

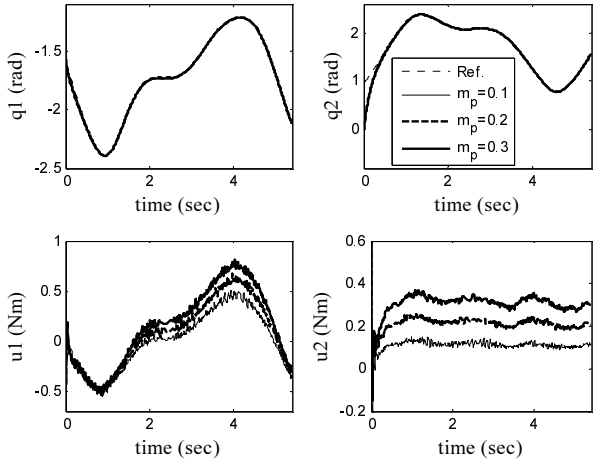

Fig. 9. Tracking responses with various payloads by the proposed control.

the proposed control, demonstrating that the compensation by the I-SDOB significantly improves the tracking precision with robustness to the constant payload uncertainty. In the Cartesian coordinate, Figs. 10-12 depict the position responses of the end effector with payloads of 0.2, 0.1, and 0.3 kg, respectively. It suggests that, as compared with the nominal control alone, the I-SDOB reduces the contour error during the transient period and effectively achieves precise trajectory tracking.

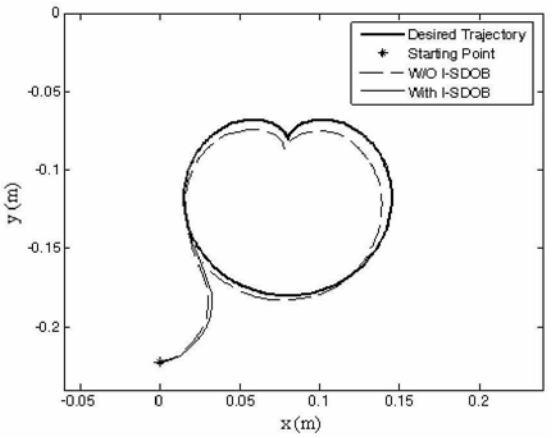

Fig. 10. Histories of the end effector with $m_p = 0.2$.

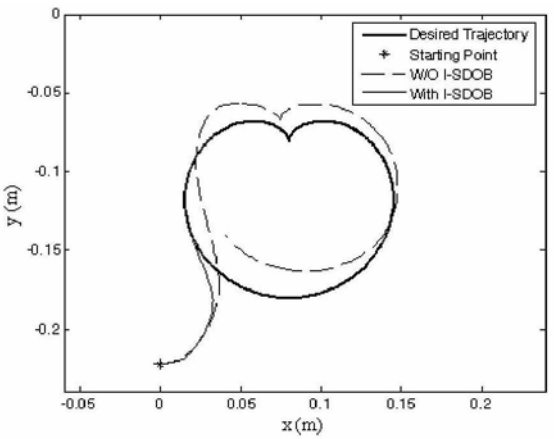

Fig. 11. Histories of the end effector with $m_p = 0.1$.

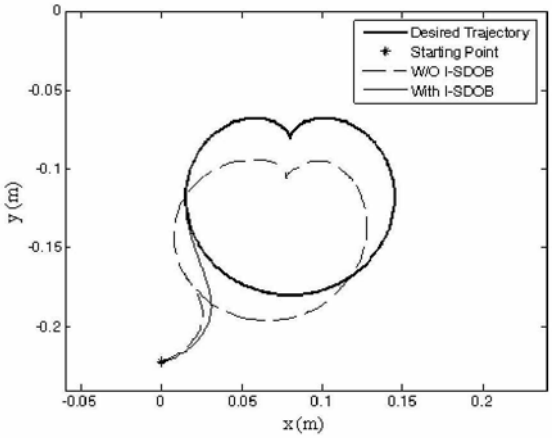

Fig. 12. Histories of the end effector with $m_p = 0.3$.

4. CONCLUSIONS

This paper presents an integral sliding disturbance observer (I-SDOB) for a class of nonlinear systems. Compared with the conventional sliding disturbance observers, the proposed I-SDOB requires only a small switching gain for guaranteeing the existence of a sliding mode, further alleviating the chatter due to the switching actions. Moreover, the stability of the overall controller-observer system is ensured using the proposed I-SDOB. The stability analysis is based on the Lyapunov theory under the assumption that the disturbance has a bounded first time derivative. In case the disturbance is constant, the proposed scheme yields global asymptotic convergence of the tracking error. Experimental results on a two-link robotic manipulator show that the proposed I-SDOB effectively compensates for unknown disturbances induced by constant payload discrepancy and improves the positioning accuracy. The introduction of the I-SDOB yields an enhanced control structure for rigid mechanical systems. Despite the success in implementing the proposed continuous-time control law in the discrete-time domain, the effect of digital implementation is not explored in this paper. Further study is required to investigate the influence of the delay due to digital implementation on the feedback system.

REFERENCES

[1] P. H. Chang and S. H. Park, "On improving time-delay control under certain hard nonlinearities," *Mechatronics*, vol. 13, pp. 393-412, 2003.

[2] S. J. Kwon and W. K. Chung, "A robust tracking controller design with hierarchical perturbation compensation," *J. Dynamic Syst. Meas. Contr., Trans. of the ASME*, vol. 124, pp. 261-271, 2002.

[3] M. Jin, S. H. Kang, and P. H. Chang, "Robust compliant motion control of robot with nonlinear friction using time-delay estimation," *IEEE Trans. on Ind. Electron.*, vol. 55, no. 1, pp. 258-269, January 2008.

[4] S. M. Shahruz, "Performance enhancement of a class of nonlinear systems by disturbance observers," *IEEE/ASME Trans. on Mechatron.*, vol. 5, no. 3, pp. 319-323, 2000.

[5] S. Katsura and K. Ohnishi, "Absolute stabilization of multimass resonant system by phase-lead compensator based on disturbance observer," *IEEE Trans. on Ind. Electron.*, vol. 54, no. 6, pp. 3389-3396, December 2007.

[6] W. Li and Y. Hori, "Vibration suppression using single neuron-based PI fuzzy controller and fractional-order disturbance observer," *IEEE Trans. on Ind. Electron.*, vol. 54, no. 1, pp. 117-126, 2007.

[7] J. Solsona, M. I. Valla, and C. Muravchik, "Nonlinear control of a permanent magnet synchronous motor with disturbance torque estimation," *IEEE Trans. on Energy Conversion*, vol. 15, no. 2, pp. 163-168, 2000.

[8] G. Zhu, L.-A. Dessaint, O. Akhrif, and A. Kaddouri, "Speed tracking control of a permanent-magnet

synchronous motor with state and load torque observer," *IEEE Trans. on Ind. Electron.*, vol. 47, no. 2, pp. 346-355, 2000.

[9] K.-H. Kim and M.-J. Youn, "A nonlinear speed control of a PM synchronous motor using a simple disturbance estimation technique," *IEEE Trans. on Ind. Electron.*, vol. 49, no. 3, pp. 524-535, 2002.

[10] H.-N. Lin and Y. Kuroe, "Decoupling control of robot manipulators by using variable-structure disturbance observer," *Proc. of the 21st Intern. Conf. on Industrial Electronics, Control, and Instrumentation*, Paris, pp. 1266-1271, November 1995.

[11] X. Chen, S. Komada, and T. Fukuda, "Design of a nonlinear disturbance observer," *IEEE Trans. on Ind. Electron.*, vol. 47, no. 2, pp. 429-437, 2000.

[12] J. T. Moura, H. Elmali, and N. Olgac, "Sliding mode control with sliding perturbation observer," *J. Dynamic Syst. Meas. Contr., Trans. of the ASME*, vol.119, pp. 657-665, 1997.

[13] Y.-S. Lu and J.-S. Chen, "Design of a perturbation estimator using the theory of variable-structure systems and its application to magnetic levitation systems," *IEEE Trans. on Ind. Electron.*, vol. 42, no. 3, pp. 281-289, 1995.

[14] V. I. Utkin, J. Guldner, and J. Shi, *Sliding Mode Control in Electromechanical Systems*, Taylor & Francis, 1999.

[15] P. Korondi, K. D. Young, and H. Hashimoto, "Sliding mode based disturbance compensation for motion control," *Proc. of the 23rd Intern. Conf. on Industrial Electronics, Control, and Instrumentation*, New Orleans, pp. 73-78, November 1997.

[16] K. D. Young, V. I. Utkin, and U. Ozguner, "A control engineer's guide to sliding mode control," *IEEE Trans. on Contr. Syst. Techn.*, vol. 7, no. 3, pp. 328-342, 1999.

[17] V. I. Utkin, *Sliding Modes and Their Application in Variable Structure Systems*, MIR, Moscow, Russia, 1978.

[18] Y.-S. Lu and C.-M. Cheng, "Design of a non-overshooting PID controller with an integral sliding perturbation observer for motor positioning systems," *JSME International Journal, Series C*, vol. 48, no. 1, pp. 103-110, March 2005.

Yu-Sheng Lu received his B.S. degree in Mechanical and Electrical Engineering from National Sun Yat-Sen University, Kaohsiung, Taiwan, in 1990, and his Ph.D. degree in Engineering from National Tsing Hua University, Hsinchu, Taiwan, in 1995. From 1997 to 1998, he was with the Electronics and Optoelectronics Research Laboratories (formerly Opto-Electronics and Systems Laboratories), Industrial Technology Research Institute, Taiwan. From 1998 to 2000, he was a Postdoctoral/Scientific Employee with the Institute of Robotics and Mechatronics, DLR, Germany. From 2000 to 2008, he was with the Department of Mechanical Engineering, National Yunlin University of Science and Technology, Yunlin, Taiwan. In 2008, he moved to the Department of Mechatronic Technology, National Taiwan Normal University, Taipei, Taiwan, where he is currently a Professor. His research interests include sliding-mode control and intelligent control with applications to mechatronic systems.

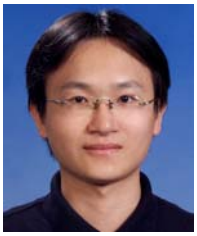

Chien-Wei Chiu was born in Taiwan on Feb. 20, 1981. He received his M.S. degree in Mechanical Engineering from National Yunlin University of Science and Technology, Yunlin, Taiwan, in 2006. He is currently a research and design engineer at the Foxconn Technology Group, Taiwan, and his research interests include robot control systems.